Uncertainty Assessment of Prognostics of Electronics Subject to Random Vibration

Jie Gu, Donald Barker and Michael Pecht

Prognostics and Health Management Lab, Center for Advanced Life Cycle Engineering (CALCE)
University of Maryland, College Park, MD 20742, USA
E-mail: jiegu@calce.umd.edu

Abstract

This paper presents a method for uncertainty analysis of prognostics with a focus on electronics subject to random vibration. First we identify uncertainty sources and types: measurement uncertainty, parameter uncertainty, failure criteria uncertainty, and future usage uncertainty. Next, we present an approach to determine the uncertainty in a prognostic analysis. Our approach utilizes a sensitivity analysis to identify the dominant input variables that influence the model output. With information of the input parameter variable distributions, a Monte Carlo simulation provides a distribution of accumulated damage. From the accumulated damage distributions, the remaining life can then be predicted with confidence intervals.

A case study is presented whereby prognostics with uncertainty is applied to an electronic circuit board subject to random vibration. The results show that the experimentally measured failure time is within the bounds of the uncertainty analysis prediction.

Introduction

Prognostics is a method that permits an assessment of the reliability of a system under its actual application conditions [1]. It can be employed by integrating sensor data with models that enable in-situ assessment of the extent of deviation or degradation of a product from an expected normal operating condition (that is, the system's "health") and also predict the future state of reliability based on historic conditions and current trends.

Prognostics has been developed and implemented in electronics in recent years. Ramakrishnan et al. [2] and Mishra et al. [3] used a physics-of-failure (PoF) approach to perform prognostics on electronics subject to various loading conditions. Gu [4] assessed prognostics subject to random vibration, but, the effect of uncertainty and of variability in the material properties and prediction procedures were not considered at that time.

For logistics use of prognostics, it is necessary to identify the uncertainties in the prognostic approach and assess the impact of these uncertainties on the remaining life distribution in order to make risk-informed decisions. Therefore, this paper addresses the uncertainty analysis of prognostics, with a case study of an electronic circuit board assembly subjected to random vibration.

In this paper, an approach is developed to assess the impact of uncertainties in measurement, parameter inputs, failure criteria, and usage on remaining life prognostics. This approach utilizes sensitivity analysis to identify the dominant input variables that influence the model output, and uses the distribution of input parameter variables in a Monte Carlo simulation to provide a distribution of accumulated damage. From accumulated damage distributions, the remaining life is then predicted with confidence intervals. The method was demonstrated using an experimental setup for predicting failures of an electronic circuit board assembly subjected to random vibration.

Experiment Setup and Uncertainty Propagation

An electronic circuit board assembly was mounted on a vibration shaker that can excite random vibration, as shown in Figure 1. The response (bending curvature) of the printed circuit board (PCB) to vibration loading was monitored using strain gauges. A strain gauge was also attached to the backside of the PCB underneath certain components to measure specific local PCB response.

An analytical model was developed to calculate the interconnect strain using the measured PCB bending curvature (and strain) [4]. The interconnect strain was then used to assess damage due to vibration failure fatigue. The damage estimates were accumulated using Miner's rule and then used to predict the life consumed and remaining life.

The model results were compared to the experimental component interconnect failures by monitoring the components' resistance. In this study, a BGA352 (one kind of ball grid array) component was analyzed to demonstrate the uncertainty implementation approach.

The uncertainty propagation for the whole prediction process is shown in Figure 2. Strain inaccuracy comes from the strain measurement on the PCB. The uncertainty

Copyright © 2007, Association for the Advancement of Artificial Intelligence (www.aaai.org). All rights reserved.

of load stress analysis comes from the model, which is used to calculate the solder strain from the PCB strain. This includes the variability of material properties and geometries. Bin width uncertainty comes from the signal processing to perform data reduction. Material fatigue constant uncertainty comes from the fatigue model used. Failure criteria and future usage uncertainty come from the assessment of the remaining life prediction from accumulated damage.

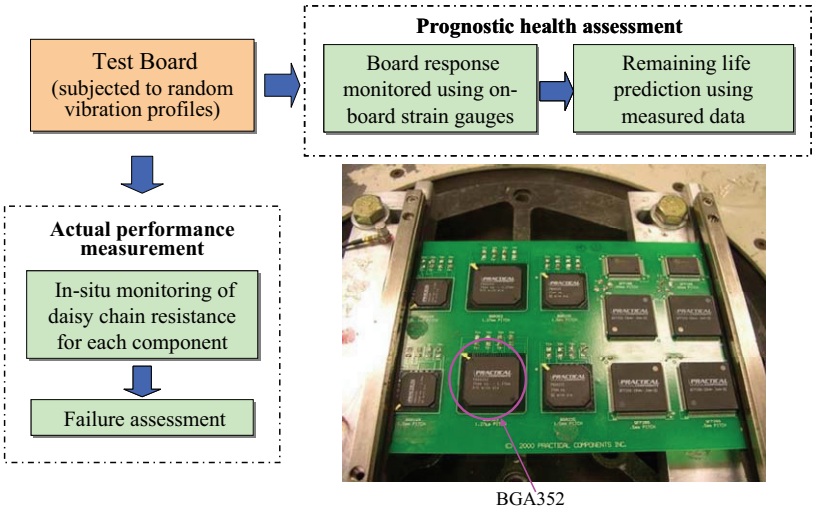

Figure 1. Prognostics of electronics under vibration loading

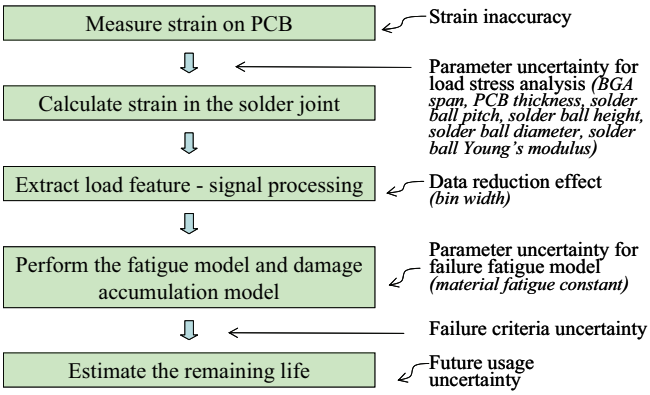

Figure 2. Uncertainty propagation

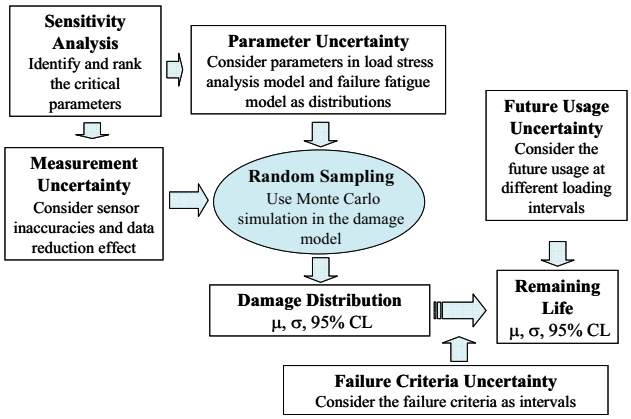

Figure 3. Uncertainty analysis for prognostics

Uncertainty Implementation Approach

The overall approach to implementing uncertainty is shown in Figure 3. The uncertainties shown in Figure 2 are categorized into four types: measurement uncertainties, parameter uncertainties, failure criteria uncertainties and future usage uncertainty (to be explained later). Critical parameters are selected from a sensitivity analysis and assigned a suitable probability density function (PDF).

In this study, random sampling by the Monte Carlo simulation method is used to assess how measurement uncertainty and parameter uncertainty affect the prediction results. The failure criteria and future usage uncertainty is considered in the remaining life assessment.

Uncertainty Source and Categorization

Four types of uncertainties and their sources are detailed discussed in this paragraph.

Measurement Uncertainty

Measurement uncertainty can be divided into two parts. One is sensor inaccuracy and the other is the data reduction effect.

Strain gage sensor inaccuracies come principally from adhesive thickness, Wheatstone bridge nonlinearity, and misalignment of strain gauges. Sometimes the adhesive depends on the curing temperature, and then the resistance can shift as much as 2 percent. If it does not depend on the curing temperature, then the resistance shift can be 0.5

percent [8]. The PCB thickness is proportional to the strain measurement, so when the PCB is very thin, the adhesive thickness will become a concern. The thickness of the PCB in this test is 1.829 mm, and the adhesive thickness is 0.05 mm, so we calculate a worst case scenario of 2.7 percent error when considering the full adhesive thickness (0.05/1.829). Errors due to Wheatstone bridge nonlinearity can be as much as 0.1 percent when the strain level is below 1,000 με [9]. Misalignment will also cause strain inaccuracy. A 5° error in mounting the rosette produces a 0.68 percent error [10]. In our test, the adhesive did not depend on the curing temperature. When the possible errors were added together, the total was about 4 percent (0.5+2.7+0.1+0.68). In addition, Vishay technique notes [11] show the error of strain gauge used in this study is normally in the range of 2 to 5 percent, so 4 percent is a reasonable value for the strain inaccuracy in this study.

During cycle counting, the vibration loads are stored in appropriate bins to achieve data reduction. Smaller bin widths may present too many details (under smoothing) and larger bin widths may present too few (over smoothing). The optimal bin width needs to be selected. However, the optimal bin width calculation also depends on the load distribution [6]. The equations to calculate the optimal bin width for the normal distribution and non-normal distribution [6][7] show a 5 percent difference. This will be counted as an uncertainty source when performing data reduction, since we do not know the real life load distribution (normal distribution or not normal distribution) in advance.

Parameter Uncertainty

Parameter uncertainty can be further divided into two parts: the load stress analysis model and the failure fatigue model.

Load stress analysis is used to calculate the material stress or strain concentration from the environmental loading. This study calculates the solder strain from PCB strain. The uncertainty arises due to variability in the material and geometric parameters that are used in the stress analysis model [4], as shown in Equation 1,

$$\varepsilon_{solder} = f(\varepsilon_{PCB}, t_{PCB}, L_{BGA}, P_{BGA}, h_{solder}, D_{soldrer}, E_{solder}) \quad (1)$$

where ε_{solder} is the calculated solder strain, ε_{PCB} is the measured PCB strain, t_{PCB} is the thickness of the PCB, L_{BGA} is the BGA span, P_{BGA} is the BGA pitch, h_{solder} is the height of the solder ball, D_{solder} is the solder ball diameter, and E_{solder} is the Young's modulus of the solder. (All the uncertainties coming from these material properties or geometries will be documented and referenced in Table 1.)

The uncertainty from the failure fatigue model arises due to the variability of the fatigue constant in the S-N curve (stress against the number of cycles-to-failure curve; see Figure 4).

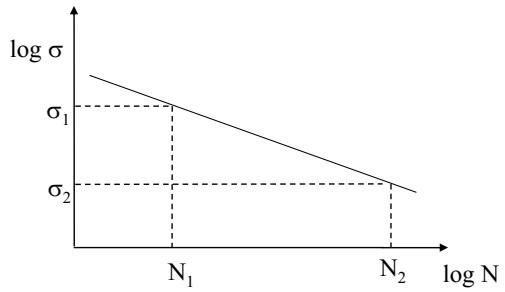

Figure 4. S-N curve

From Basquin's model,

$$\sigma_1^{\,b} N_1 = \sigma_2^{\,b} N_2 \quad (2)$$

where b is the fatigue constant. For this constant, Steinberg [12] is using 6.4, while the military [13] is using 4. The slope of the S-N curve is -1/b. When we consider the variability of b by changing the slope of the S-N curve, one assumption is that the S-N curve is always passing one point (N: 100,000, σ : 4.8MPa [15]). That is because the combination of the slope and one point can identify one line. The reason for choosing this point is to make sure the result will be reasonable in the accelerated testing conditions for comparison purposes.

Failure Criteria Uncertainty

From Miner's rule in Equation 3, the damage fraction (D) at any stress level is assumed to be linearly proportional to the ratio of the number of cycles of operation (n_i) to the total number of cycles that would produce failure (N_i) at that stress level. When the summation of all the D (D_{total}) is larger than 1, failure is considered to have occurred. However, safety margins may be taken into consideration in some situations. In addition, the loading sequences can affect the results [5], so it is necessary to consider the failure criteria as an interval rather than one single data point. The literature [5] indicates the failure criteria value for D_{total} can change from 0.5 to 2.

$$D_{total} = \sum_{i=1}^{n} \frac{n_i}{N_i} \quad (3)$$

Future Usage Uncertainty

When we carry out uncertainty analysis, the assessment is based on the current and historical data points. The future usage is assumed to be the same loading level as the previous overall usage. However, in reality, the future usage profile or mission may vary from the previous one. For example, the product may be in storage for a while, or the next mission may be different than the previous one. Variables as these will affect the prediction results.

Sensitivity Analysis

Sensitivity analysis was conducted for the parameters listed above. First the input parameters listed in column 1 of Table 1 were changed by 1 percent to see how they affect the results, and the results were ranked (see column 4 of Table 1). However, some parameters may change more than 1 percent, while others change less. For example, some parameters (PCB thickness, BGA span, solder ball pitch, solder ball height and solder ball diameter) were considered to be normally distributed in this study. Meanwhile, the solder ball Young's modulus is a temperature-dependent parameter, changing due to the environment and operational system, so a uniform distribution was assigned to represent temperature randomness. The fatigue model constant, bin width effect, and strain measure inaccuracy were also assigned uniform distributions. Percentage changes of damage accumulation for one hour due to the tolerance/range of input parameters (based on the assigned distributions) were calculated and are shown in column 6 of Table 1. The percentage changes are due to the maximum and minimum x values shown in column 5. The updated rank (column 7 of Table 1) from these changes shows a significant difference from the previous rank, so it is necessary to consider the actual parameter tolerance in the sensitivity analysis.

Table 1. Sensitivity analysis for input parameters

Input parameters (x_i)	Mean	Percentage change of one hour damage accumulation due to 1% change of x_i	Rank	Tolerance /Range	Percentage change of one hour damage accumulation due to tolerance/range of x_i	Updated rank
BGA span	31.75 (mm)	22.0%	1	+/- 0.25	16.8%	8
PCB thickness	1.829 (mm)	6.1%	6	+/- 0.15	39.6%	4
Solder ball pitch	1.27 (mm)	7.1%	3	+/- 0.04	21.8%	7
Solder ball height	0.52 (mm)	6.2%	5	+/- 0.05	44.4%	3
Solder ball diameter	0.76 (mm)	12.4%	2	+/- 0.05	57.0%	2
Solder ball Young's modulus	29914 (MPa) (303K)	1.8%	8	25354 (333K) 34474 (273K)	22.4%	6
Fatigue model constant: b	6.4	5.9%	7	- 2	598.1%	1
Data bin width	Optimal	0.3%	9	+/- 5%	1.8%	9
Strain measurement	NA	6.6%	4	+/- 4%	28.4%	5

Monte Carlo Simulation for Measurement and Parameter Uncertainty

Based on the updated rank in Table 1, the first five parameters' uncertainties were considered critical, thus they were selected to assess the uncertainty of the remaining life prediction. The solder ball diameter and height are dependent on each other. When two parameters are coupled, the following steps can be used to generate the distributions: first, let the two distributions that are correlated be f(x) and f(y); then calculate the correlation coefficient, ρ , from equations 4 through 7; after that, random sample for f(x) distribution N times to get X = $\{x_1, x_2, \ldots x_N\}$; then calculate y_i for each value of x_i based on ρ and variance in x and y using Equation 8; last, use new pairs of (x_i, y_i) together in the Monte Carlo simulation.

$$\rho = \frac{\mathrm{cov}(x,y)}{S_x S_y} \tag{4}$$

$$\mathrm{cov}(x,y) = \frac{\sum (x_i - \bar{x})(y_i - \bar{y})}{n-1} \tag{5}$$

$$S_x = \sqrt{\frac{\sum (x_i - \bar{x})^2}{n-1}} \tag{6}$$

$$S_y = \sqrt{\frac{\sum (y_i - \bar{y})^2}{n-1}} \tag{7}$$

$$\hat{y} = \frac{\rho S_y}{S_x}(x - \bar{x}) + \bar{y} \tag{8}$$

where S_x and S_y are the variance of f(x) and f(y).

In this study, the relation between solder ball diameter (D) and solder ball height (h) is shown in Equation 9, in which the solder volume, V, was fixed. The solder ball height (h) was calculated from the solder ball diameter (D) when the solder volume was known. However, solder volume was also a variable; therefore a distribution was also assigned for the volume. That is to say, the first two independent distributions were generated: one for solder ball diameter and the other for solder ball volume. Then the solder ball height was calculated using random numbers from those two distributions. Finally, the solder ball diameter and solder ball height were used in the Monte Carlo simulations.

$$V = f(D,h) \tag{9}$$

The stopping criterion for the Monte Carlo simulation is based on minimizing the variance over the mean of the simulation results. For example, if, d_1, d_2, …d_m are the results of the simulation, then the simulation stopped when:

$$\frac{\sigma}{\sqrt{m}} \le 0.01\mu \qquad (10)$$

Here, the mean, variance, and standard error over the mean are calculated as follows:

$$\sigma^2 = \frac{1}{m-1}\sum_{i=1}^{m}(d_i - \mu)^2 \qquad (11)$$

$$\mu = \frac{1}{m}\sum_{i=1}^{m} d_i \qquad (12)$$

The five most critical parameters (PCB thickness, solder ball diameter, solder ball height, failure fatigue constant, and strain measurement) were selected for uncertainty analysis. The probability density function (PDF) was assigned for each parameter as shown in Figure 5. These distributions were input into a Monte Carlo simulation. In Figure 5, the mean value of accumulated damage in one hour became stable when the Monte Carlo sample size was increased, and Equation 10 was used to control the simulation sample size.

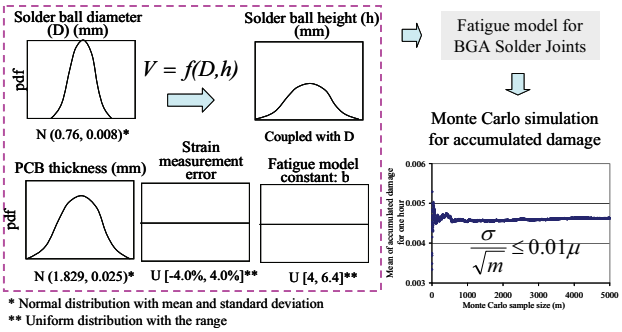

Figure 5. Input parameters for Monte Carlo simulation

Figure 6 shows the distribution of the accumulated damage in the first hour. Lognormal is the most suitable distribution to fit the data in this case The mean value of the distribution is 0.00464, and the upper and lower limit bound was calculated for a 95 percent confidence level. A similar distribution was obtained for each hour that followed. The total damage distribution was calculated by adding together the damage distributions for each previous hour, as shown in Figure 7. When the damage accumulates with time, the uncertainty also accumulates with time. Five different failure probability curves were used to present how the damage and uncertainty accumulated: 1 percent, 5 percent, 50 percent, 95 percent and 99 percent. The uncertainty becomes wider as the time increases. One percent probability implies much faster failure than 99 percent. Figure 8 shows the remaining life prediction based on the different failure probabilities. The remaining life calculation is performed using Equation 13 [4]. The actual failure point is between 50 percent and 95 percent of the failure probability. In addition, the predictions based on 1 percent failure probability and 99 percent failure probability involve around ten hours difference. Then,

$$RL_N = \frac{N}{DR_N} - N \qquad (13)$$

where RL_N is the remaining life at the end of N hour, and DR_N is the damage ratio accumulated at the Nth hour.

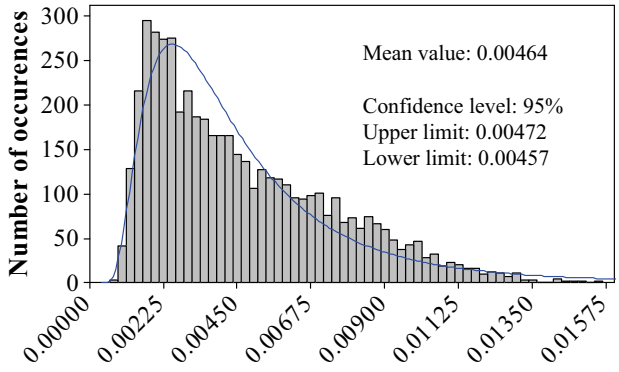

Figure 6. Accumulated damage distribution for one hour

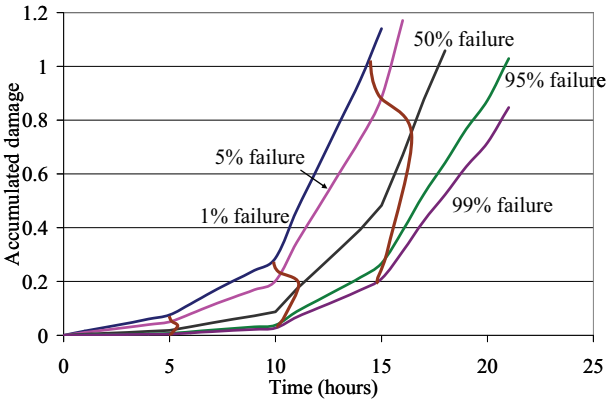

Figure 7. Damage accumulation

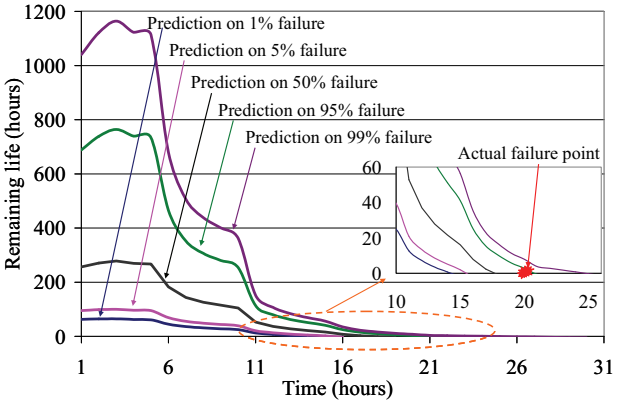

Figure 8. Remaining life prediction

Prediction Considering Failure Criteria Uncertainty

Failure criteria will be affected by the loading sequence and safety concerns. If the application involves human participation (such as aircraft or spacecraft) or may compromise the safety of personnel (such as machinery in a factory), a lower limit of damage accumulation may be chosen, but if the application is known to be fairly reliable (such as for systems with multiple redundancy), a higher limit of damage accumulation may be selected. Three different levels (see Table 2) were considered because of different safety concerns. When a given level was selected for the application, the predicted remaining life bounds were calculated with failure probability. In this study, 50 percent failure probability was used; the prediction results are shown in Table 3. The lower/upper bound in Table 3 is the bound for the input interval in Table 2. For example, when the failure criteria interval is from 0.5 to 1, the predicted life can be from 15.09 to 17.68 hours. When there is less concern for safety, predicted remaining life can increase. The different failure criteria will not only affect the final prediction point, they will also affect the prediction from the beginning, as shown in Figure 9.

Table 2. Failure criteria categorization

Safety concern	High	Normal	Low
Accumulated damage to failure	0.5 – 1.0	1.0 – 1.5	1.5 – 2.0

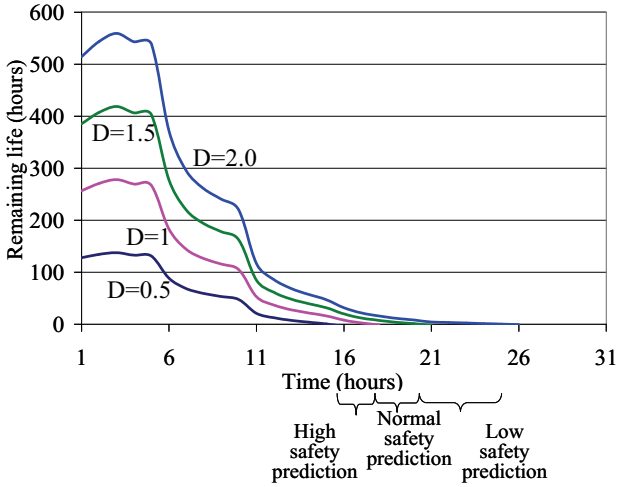

Figure 9. Prediction considering failure criteria uncertainty

Table 3. Remaining life prediction considering failure criteria uncertainty

Safety issue	Remaining life prediction (hours) on 50% probability failure	
	Lower bound	Upper bound
High	15.09	17.68
Normal	17.68	20.34
Low	20.34	25.36

Prediction Considering Future Usage Uncertainty

Normally the prediction of reliability (remaining life) is based on the overall damage from the current and historical data and trends. If the future usage data is different from the historical usage profile, then the prediction will become inaccurate. Therefore, it is necessary to consider the variability of the future usage profiles.

In our case we consider three levels: a low loading condition, a normal loading condition and a high loading condition, with corresponding input PSD levels (see Table 4). A prediction was made at the tenth hour based on different usage levels, as shown in Table 5. The lower/upper bound of remaining life corresponds to the input PSD intervals. For example, in the normal loading condition (PSD from 0.1 to 0.3 G^2/Hz), the predicted remaining life is from 4.86 to 66.32 hours. The "0" in Table 5 occurs if there is sudden shock loading, while "infinite" means the product is not in use. Figure 10 shows how future usage loading data can affect the prediction results. This analysis can help evaluate whether the product is suitable for the next mission or for a couple of times. Of course, since the loading conditions may change, in-situ prediction is preferred and can give more accurate results.

Table 4. Loading level for future usage

Future usage	Low loading	Normal loading	High loading
Input PSD level (G^2/Hz)	0 – 0.1	0.1 – 0.3	> 0.3

Table 5. Remaining life prediction considering future usage

Future usage profile	Remaining life prediction (hours) of 50% probability failure at the 10th hour	
	Lower bound	Upper bound
Low loading	66.32	Infinite
Normal loading	4.86	66.32
High loading	0	4.86

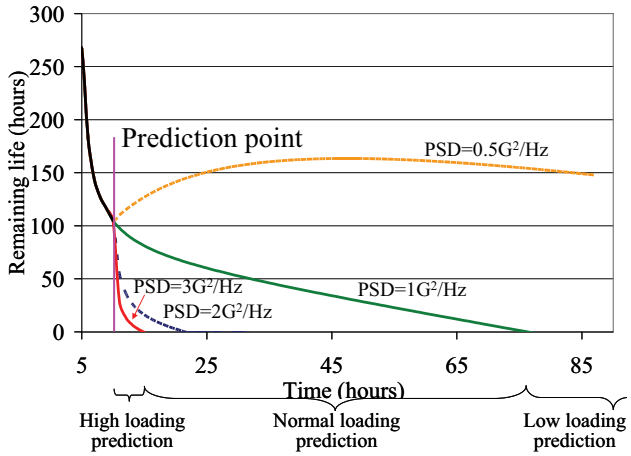

Figure 10. Prediction considering future usage uncertainty

Uncertainty Range

Figure 8 shows the difference between a 1 percent failure probability and a 99 percent failure probability on remaining life prediction. The range of the two predictions is wide; thus, the uncertainty is quite large. This makes decision-making difficult. In order to narrow down the uncertainty, first, the uncertainty should be measured quantitatively for comparison purposes. The definition of the uncertainty range is the distance between the 1 percent point and the 99 percent point in the uncertainty distribution. (Figure 11 gives the schematic explanation.) Then, all uncertainty sources can be checked to determine which parameter(s) or step(s) contribute most to the final uncertainty.

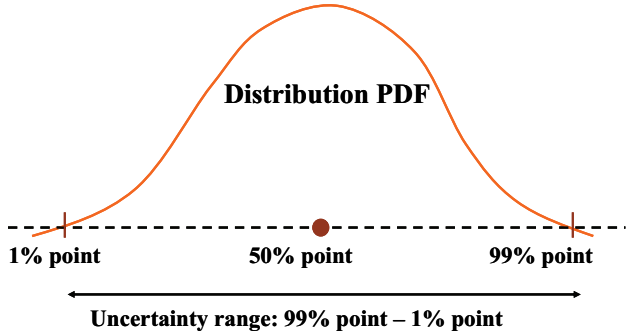

Figure 11. Uncertainty range

The damage range for each parameter or each step based on damage accumulated in the sixteenth hour is shown in Figure 12. When an individual parameter was considered, such as the PCB thickness, it was considered as an input distribution, while other parameters were given a single value. The length of the individual bar in the figure is the damage range for certain parameters, and the solid dot is the 50 percent probability point. In this analysis, the solder ball diameter and solder ball height were considered as coupled parameters, so the analysis was performed at the same time. This was also the case for the solder ball pitch and BGA span. In Figure 12, the load stress analysis parameters include solder ball pitch, BGA span, PCB thickness, solder ball diameter, solder ball height, and Young's modulus of the solder. The result shown in Figure 12 is also summarized in Table 6. The straight line in Figure 12 represents the predicted damage in the sixteenth hour without considering the uncertainty calculations. In many cases, the 50 percent probability failure point would be on that straight line.

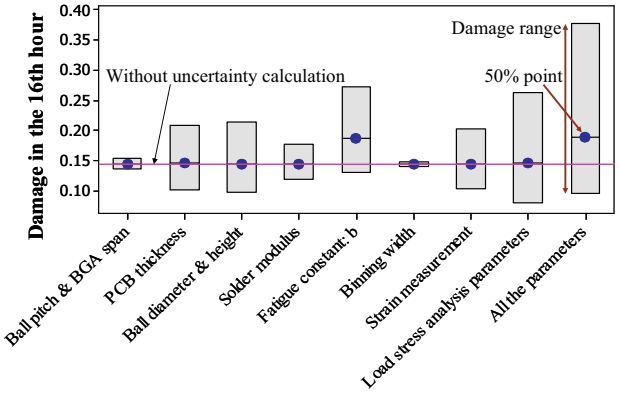

Figure 12. Damage range for the sixteenth hour

In Table 6, the second column is the damage range for each parameter or the step corresponding to Figure 12. The third column gives the rank for these parameters. The fatigue constant was found to be the most critical parameter in this uncertainty analysis. In real life, the fatigue constant will contribute even more. Since the damage range caused by the fatigue constant variation will be magnified by the acceleration factor when considering the real life loading condition compared to this accelerated test condition. Therefore, to reduce the uncertainty, the failure fatigue model must first be improved to get a more accurate material fatigue constant. Then, the product quality must be considered to reduce the tolerance of the parameters for material properties and geometries, as well as to increase the sensor measurement accuracy.

Load stress analysis parameters include solder ball pitch, BGA span, PCB thickness, solder ball diameter, solder ball height, and Young's modulus of the solder. If they are considered separately as input and then added together, the damage range is 0.299 (0.017+0.107+0.117+0.059). When they are considered together as a whole for uncertainty analysis input, the damage range is 0.182, which is smaller than 0.299. That is to say, the sum of the individual uncertainty ranges is larger than when they are considered all together. This is also the case when all the parameters are considered separately and together. One possible explanation is that the individual uncertainties may counteract each other.

The other observation is that the rank for the damage range is similar to the sensitivity analysis rank. Therefore, it is reasonable to assume that the first five parameters from the sensitivity analysis should be used to perform the

uncertainty analysis, since they contribute the most to the final uncertainties.

Table 6. Damage range and rank for the 16th hour

Parameters	Damage range	Rank
Ball pitch & BGA span	0.017	6
PCB thickness	0.107	3
Ball diameter & height	0.117	2
Solder modulus	0.059	5
Fatigue constant: b	0.142	1
Bin width	0.008	7
Strain measurement	0.099	4
Load stress analysis parameters	0.182	
All the parameters	0.283	

Conclusions

In this paper, an approach for applying uncertainty analysis to physics-of-failure-based prognostics has been provided. The approach utilizes sensitivity analysis to identify the dominant input variables that influence the model-output, and uses the distributions of input variables in a Monte-Carlo simulation to provide a distribution of accumulated damage. Given the measurement, parameter, failure criteria, and future usage uncertainty, the actual failures in testing were observed to occur within the predicted failure distribution. The sensitivity analysis procedure revealed that it is important to consider the tolerances of the parameter variables, as they can strongly influence the ranking of the most sensitive variables. Uncertainty propagation and uncertainty ranges were also discussed. It was determined that the fatigue constant is a key contributor to uncertainty. Based on the uncertainty assessment, the prognostic approach enables the user to make remaining life predictions with fewer data sets, and initial rough estimates can be made before the entire model parameters are collected, or any future loading is recorded. The estimates are valuable for initial planning. When sufficient usage data and model parameters are available; the estimates will provide more accurate predictions that enhance decision making. It was observed that the prediction accuracy increased with a decrease in the remaining life of the product. This was attributed to the fact that with increased usage there was more data to support the prognostics.

References

[1] Vichare, N., and Pecht, M. 2006. Prognostics and Health Management of Electronics. *IEEE Transactions on Components and Packaging Technologies* 29(1): 222–229.

[2] Ramakrishnan, A., and Pecht, M. 2003. A Life Consumption Monitoring Methodology for Electronic Systems. *IEEE Transactions on Components and Packaging Technologies* 26(3): 625–634.

[3] Mishra, S., Pecht, M., Smith, T., McNee, I., and Harris, R. 2002. Remaining Life Prediction of Electronic Products using Life Consumption Monitoring Approach. *Proceedings of the European Microelectronic Package Interconnection Symposium*, 136–142.

[4] Gu, J., Barker, D., and Pecht, M. Prognostics Implementation of Electronics Under Vibration Loading. Accepted by the *Journal of Microelectronic Reliability.*

[5] Sobczyk, K., and Spencer, B.F. 1992. *Random Fatigue: From Data to Theory*. Boston, MA: Academic Press, Inc.

[6] Vichare, N., Rodgers, P., and Pecht, M. 2006. Methods for Binning and Density Estimation of Load Parameters for Prognostics and Health Management. *International Journal of Performability Engineering* 2(2): 149-161.

[7] Izenman, A.J. 1991. Recent Developments in Non Parametric Density Estimation. *Journal of American Statistical Association* 86(413): 205-213.

[8] Vishay Technical Articles, 2005, Quality Control of Strain Gauge Installations, Vishay Inc.

[9] Vishay Technique Note, 2005, Errors Due to Wheatstone Bridge Nonlinearity, TN-507-1, Vishay Inc.

[10] Vishay Technique Note, 2005, Errors Due to Misalignment of Strain Gages, TN-511, Vishay Inc.

[11] Vishay Technique Note, 2005, Strain Gage Selection - Criteria, Procedures, Recommendations, TN-505-4, Vishay Inc.

[12] Steinberg, D. 2000. *Vibration Analysis for Electronic Equipment, third edition.* New York: John Wiley & Sons, Inc.

[13] Mil-Std-810 Section 514.4: Accelerated Testing.

[14] Lau, J.H., and Liu, K. 2004. Global Trends in Lead-free Soldering, Part II. *Advanced Packaging* 13(2): 25-28.

[15] Kim, Y.B., Noguchi, H., and Amagai, M. 2006. Vibration Fatigue Reliability of BGA-IC Package with Pb-free Solder and Pb–Sn Solder. *Journal of Microelectronics Reliability* 46: 459–466.